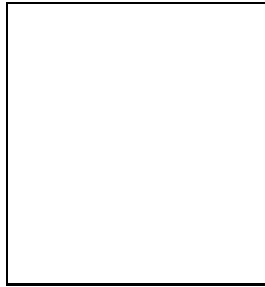


**XIth International Conference on
Elastic and Diffractive Scattering
Château de Blois, France, May 15 - 20, 2005**

THE ALICE DETECTOR AT LHC

R. SCHICKER

*Phys. Inst., University Heidelberg, Philosophenweg 12,
69120 Heidelberg, Germany*



The ALICE experiment at the Large Hadron Collider LHC is presented, and an overview of its physics program is given. A few specific observables are discussed in order to illustrate the physics potential of ALICE.

1 Introduction

The ALICE experiment is a general purpose heavy ion experiment to study the behaviour of strongly interacting matter at LHC energies. The behaviour of such matter addresses both equilibrium and non-equilibrium physics in an energy density region of $\varepsilon \sim 1\text{-}1000 \text{ GeV}/\text{fm}^3$. This range includes the energy densities at which phase transitions of strongly interacting matter occur representing sudden changes of the nonperturbative vacuum structure. Of particular interest are the deconfinement transition and the restoration of chiral symmetry. Even though the two transitions are related to different aspects of the QCD vacuum, both are closely connected at the critical temperature T_c . A plethora of experimental observables is expected to indicate the onset of these phase transitions. It is the goal of the ALICE experiment to establish signatures of these transitions.

Nucleus-nucleus collisions at LHC open up a new domain. The available nucleon-nucleon center of mass energy as compared to RHIC is larger by a factor of about 30. ALICE will probe parton distributions at values of Bjorken- x as low as 10^{-5} . At these values, the gluon density is thought to be close to phase space saturation, and strong nuclear gluon shadowing is expected.

2 The ALICE detector

ALICE is designed as a general purpose experiment with a central barrel and a forward muon spectrometer¹. The central barrel pseudorapidity acceptance is $|\eta| \leq 0.9$ with a magnetic field of 0.5 T. The central detectors track and identify particles from $\sim 100 \text{ MeVc}^{-1}$ to $\sim 100 \text{ GeVc}^{-1}$ transverse momenta. Short-lived particles such as hyperons, D and B mesons are identified by their reconstructed secondary decay vertex. The detector granularity is chosen such that these tasks can be performed in a high multiplicity environment of up to 8000 charged particles per unit of rapidity. Tracking of particles is achieved by the inner tracking system (ITS) of six layers of silicon detectors, a large Time-Projection-Chamber (TPC) and a high granularity Transition-Radiation Detector (TRD). Particle identification in the central barrel is performed by measuring energy loss in the tracking detectors, transition radiation in the TRD and time-of-flight in a high-resolution TOF array. A single arm High-Momentum Particle Identification Detector (HMPID) with limited solid angle coverage extends the momentum range of identified hadrons. Photons will be measured by a crystal PbWO_4 PHOTon Spectrometer (PHOS). Additional detectors close to the beam pipe define an interaction trigger. The forward muon spectrometer covers the pseudorapidity region $-4.0 \leq \eta \leq -2.5$ with a low momentum cutoff of 4 GeVc^{-1} .

3 LHC experimental conditions

The Large Hadron Collider LHC is designed to run in proton-proton, proton-nucleus and nucleus-nucleus mode. In nucleus-nucleus mode, the Pb-Pb system is considered to be most important due to the highest energy densities reached in these collisions. Lower energy densities are reached in intermediate mass systems. Taking data in proton-proton collisions has a threefold purpose. First, proton-proton collisions at LHC explore a new energy domain and contain interesting physics in its own right². Second, detector calibration is much simpler in the low multiplicity environment of proton collisions. Third, these data serve as reference for nucleus-nucleus collisions to establish medium modifications of observed quantities.

Table 1: Maximum nucleon-nucleon center of mass energy, geometric cross section, initial and time averaged luminosity for different collision systems

System	\sqrt{s} (TeV)	σ_{geom} (b)	\mathcal{L}_0 ($\text{cm}^{-2}\text{s}^{-1}$)	$\mathcal{L}/\mathcal{L}_0$
Pb-Pb	5.5	7.7	1.0×10^{27}	0.44
Ar-Ar	6.3	2.7	1.0×10^{29}	0.64
O-O	7.0	1.4	2.0×10^{29}	0.73
p-p	14.0	0.07	5.0×10^{30}	

Table 1 lists center of mass energies and expected luminosities for some systems which will be measured by ALICE. The time averaged luminosity \mathcal{L} depends on machine filling time, experiment setup time, beam lifetime and initial beam luminosity \mathcal{L}_0 . The electromagnetic cross section of $\sigma \sim 500 \text{ b}$ limits the lifetime of the Pb beams to about 7 or 4 hours for one or two data taking experiments, respectively. First pp collisions will be measured during the commissioning of the LHC. Pb-Pb collisions are expected at the end of the first pp run.

4 The ALICE physics program

The ALICE experimental program spans a wide range of physics topics pertinent to the understanding of strongly interacting matter². Due to limitation in scope of this contribution, I have chosen three different topics in order to illustrate the ALICE physics potential.

4.1 Multiplicity distribution

The average charged particle multiplicity per unit of rapidity dN_{Ch}/dy is one of the first observables which will be measured at LHC start-up. Since the multiplicity is related to the entropy density and hence to the energy density, it affects the calculation of most other observables. Despite the fundamental importance, there is so far no ab initio calculation of particle multiplicity starting from the QCD Lagrangian. The particle multiplicity is driven by soft non-perturbative QCD, and the relevant processes must be modelled by the new scale $R_A \sim A^{1/3}$ fm.

The inclusive hadron rapidity density in $pp \rightarrow hX$ is defined to be

$$\frac{dN_{Ch}}{dy} = \frac{1}{\sigma_{in}^{pp}(s)} \int_0^{p_t^{max}} dp_t^2 \frac{d\sigma^{pp \rightarrow hX}}{dy dp_t^2}, \quad (1)$$

The pp inelastic cross section σ_{in}^{pp} grows at energies $\sqrt{s} > 20$ GeV. The energy dependence is, however, poorly known, and can be parametrized by either logarithmic or power law behaviour. Extrapolating measured pp data by such fits results in an extrapolated rapidity density in pp collisions of about 5 at energies relevant for ALICE³.

The multiplicity in central nucleus-nucleus collisions at LHC energies can be estimated by dimensional arguments. A saturation scale Q_s is assumed which represents the transverse density of all particles produced within one unit of rapidity

$$\frac{N}{R_A^2} = Q_s^2 \quad (2)$$

where $R_A = A^{1/3}$ fm and proportionality factors are set to unity.

In central nucleus-nucleus collisions, at scale Q_s , we have

$$N = \frac{A^2}{R_A^2} \frac{1}{Q_s^2} \quad (3)$$

with the factors A^2/R_A^2 stemming from the nuclear overlap function and $1/Q_s^2$ from the subprocess cross section.

Eqs. 2 and 3 can be combined with $R_A = A^{1/3}$ fm

$$N = A = Q_s^2 R_A^2 \rightarrow Q_s = 0.2 A^{1/6} \text{ GeV}. \quad (4)$$

A more refined analysis has to include the energy dependence of Q_s , for example by a power law dependence. Models of LHC particle multiplicity need to determine the constant factors which have been set to unity in this dimensional argument.

4.2 Parton energy loss

After an energetic parton is produced in a medium by a hard collision, it will radiate energy by emitting a gluon⁴. Both the parton and the gluon traverse the medium of size L . The average energy loss of the parton in the limit $E_{parton} \rightarrow \infty$ due to gluon radiation with a spectrum $\frac{\omega dI}{d\omega}$ is given by

$$\Delta E = \int^{\omega_c} \frac{\omega dI}{d\omega} \simeq \alpha_s \omega_c, \quad \text{with} \quad \omega_c = \frac{1}{2} \hat{q} L^2 \quad (5)$$

The medium dependence of the energy loss is governed by the transport coefficient

$$\hat{q} \simeq \mu^2/\lambda \simeq \rho \int dq_{\perp}^2 q_{\perp}^2 d\sigma/dq_{\perp}^2 \quad (6)$$

with ρ the density of the medium and σ the gluon-medium interaction cross section.

The coefficient \hat{q} can be expressed by the gluon structure function, i.e. for nuclear matter

$$\hat{q} = \frac{4\pi^2\alpha_s N_c}{N_c^2 - 1} \rho [xG(x, \hat{q}L)] \quad (7)$$

with $xG(x, Q^2)$ the gluon distribution for a nucleon and ρ the nuclear density.

The energy loss of heavy quarks is expected to be reduced due to suppression of gluon radiation in a cone which scales with quark mass. The yield of inclusive large p_\perp hadrons in nucleus-nucleus collisions is modified due to the medium induced radiative energy loss. This induced energy loss leads to jet quenching. The quenching of jets can be measured by comparing spectra of particles produced in nucleus-nucleus and nucleon-nucleon collisions⁵. Moreover, particle spectra of nucleus-nucleus collisions can be analyzed with respect to the reaction plane.

4.3 Quarkonia production

The dissociation of quarkonia states is one of the most important observable for the existence of a deconfined state. The suppression of quarkonia is due to the shielding of potential by Debye screening⁶. A quantitative characterization of dissociation temperature depends on the structure of heavy quark potential which can be extracted by an analysis of heavy quark free energies on the lattice⁷. While some authors claim an abrupt J/Ψ dissociation at $T = 1.9T_c$, others conclude a rather gradual J/Ψ dissociation with complete disappearance only at $T = 3.0T_c$ ^{8,9}.

In order to be reliable probes in nucleus-nucleus collisions, the cross sections for heavy quark and quarkonia production need to be known in proton-proton collisions. Predictions for the $c\bar{c}$ -pair production cross section in pp collisions at 14 TeV range from 7 to 17 mb depending on the values used for the charm mass and for the factorization and renormalization scale¹⁰. In the case of bottom pairs in pp-collisions at 14 TeV, the different parameter sets result in $b\bar{b}$ production cross sections between 0.2 and 0.7 mb.

Nuclear absorption and secondary scatterings with comovers can break up the quarkonia states and hence reduce the expected rates. The large number of $q\bar{q}$ pairs produced at LHC energies could, however, be an abundant source of final state quarkonia by coalescence due to statistical hadronization. This mechanism could result in an enhanced J/Ψ production at LHC energies¹¹.

Acknowledgments

This work was supported in part by the German BMBF under project 06HD160I.

References

1. ALICE Technical Proposal, CERN/LHCC/95-71 (1995)
2. ALICE Physics Performance Report, Vol.I, J.Phys.G: Nucl.Part.Phys.30 (2004) 1517
3. K.J.Eskola, K.Kajantie, P.V.Ruuskanen and K.Tuominen, Nucl.Phys. B570 (2000) 379
4. R.Baier et al., Nucl.Phys. B483 (1997) 291
5. D.d'Enterria, J.Phys.G:Nucl.Part.Phys.30 (2004) 767
6. T.Matsui and H.Satz, Phys.Lett. B 178 (1986) 416
7. F.Karsch, J.Phys.G:Nucl.Part.Phys.30 (2004) 887
8. M.Asakawa and T.Hatsuda, Phys.Rev.Lett. 92 (2004) 012001
9. S.Datta, F.Karsch, P.Petreczky and I.Wetzorke, Phys.Rev. D69, (2004) 094507
10. Heavy flavour physics, Hard probes in HI collisions at the LHC, hep-ph/0311048
11. P.Braun-Munzinger and J.Stachel, Phys.Lett.B 490 (2000) 196